

# Tachyon condensation and off-shell gravity/gauge duality

Yun Soo Myung <sup>1</sup>

*Institute of Mathematical Science and School of Computer Aided Science,  
Inje University, Gimhae 621-749, Korea*

## Abstract

We investigate quasilocal tachyon condensation by using gravity/gauge duality. In order to cure the IR divergence due to a tachyon, we introduce two regularization schemes: AdS space and a d=10 Schwarzschild black hole in a cavity. These provide stable canonical ensembles and thus are good candidates for the endpoint of tachyon condensation. Introducing the Cardy-Verlinde formula, we establish the on-shell gravity/gauge duality. We propose that the stringy geometry resulting from the off-shell tachyon dynamics matches onto the off-shell AdS black hole, where “off-shell” means non-equilibrium configuration. The instability induced by condensation of a tachyon behaves like an off-shell black hole and evolves toward a large stable black hole. The off-shell free energy and its derivative ( $\beta$ -function) are used to show the off-shell gravity/gauge duality for the process of tachyon condensation. Further, d=10 Schwarzschild black hole in a cavity is considered for the Hagedorn transition as a possible explanation of the tachyon condensation.

---

<sup>1</sup>e-mail address: ysmyoung@inje.ac.kr

# 1 Introduction

In general, closed-string tachyon condensation is a difficult issue because we evaluate the string partition function on a cone which has an IR divergence. The cone is not a solution to string equations of motion. Thus, the Einstein equation is no longer satisfied unless there is a delta-function source at the tip to account for the cone curvature [1]. In this case we have to use an off-shell formalism of string theory to compute the partition function. In order to cure this, one considers string theory on an orbifold  $\mathbf{C}/\mathbf{Z}_N$  instead of a cone[2, 3, 4, 5]. Similarly, there has been progress with regards to quasilocal tachyons on this direction[6]. For this purpose, one introduces the winding tachyonic modes to a warped Scherk-Schwarz cone with topology  $S^1 \times Y$ [7]. A process of winding tachyon condensation causes the circle  $S^1$  on the cone to pinch off when the size of  $S^1$  reaches the string scale  $l_s$ , removing the large cone sector  $X$  from the small cone including the singularity[8]. We are interested in the evolution of the tachyon instability in the former sector  $X$ [9, 10], although the latter can be used to study the singularity and unitarity issues in a stringy black hole by using the tachyon condensate phase[11, 12, 13]. If the dilaton can be kept small throughout the background  $X$ , the process of closed-string tachyon condensation may be viewed either as a renormalization group (RG)-flow on the world sheets or a flow in the space of the off-shell string backgrounds.

A black hole may be in unstable equilibrium with a heat reservoir in asymptotically flat spacetime. Its fate under small fluctuations will be either to decay to a hot flat space or to grow without limit by absorbing radiation from the heat reservoir. This is known as the Gross-Perry-Yaffe (GPY) instability of a hot flat spacetime[14]. There are two ways to achieve a stable black hole in equilibrium with heat reservoir. A black hole could be rendered canonically stable by placing it in AdS space[15] or by introducing a cavity surrounding it [16]. This corresponds to the IR regularization. The canonical ensemble for quantum gravity in AdS<sub>5</sub> space can be defined by the Euclidean path integral over the metric and all other fields with the time direction periodically identified with an inverse temperature  $\beta = 1/T$ . In the semi-classical approach, the path integral is dominated by configurations near saddle points, that is, classical solutions to the Einstein equations. There are three possible on-shell string background as saddle points: thermal AdS<sub>5</sub>, a small unstable black hole (UBH), and a large stable black hole (SBH). The thermal AdS<sub>5</sub> of topology  $S^1 \times R^4$  and SBH of topology  $R^2 \times S^3$  are locally stable, while the UBH of topology  $R^2 \times S^3$  is unstable against decay. However, all of these have a common boundary of topology  $S^1 \times S^3$  on which one may define the boundary CFT.

On the strongly coupled CFT side, string theory backgrounds of a bubble, unstable

bounce (UB) and stable bounce (SB) appear as saddle points in the Euclidean path integral of  $\mathcal{N} = 4, SU(N)$  Super-Yang-Mills (SYM) theory. According to the AdS/CFT correspondence[17, 18, 19], Witten has shown that a SBH in bulk-AdS<sub>5</sub> space could be described by the deconfinement phase SB of  $\mathcal{N} = 4$  SYM theory on  $S^1 \times S^3$ [20]. Further the Hawking-Page transition corresponds to a large  $N$  deconfinement/confinement transition in the strongly coupled gauge theory. On the other hand, the UB undergoes the Gross-Witten phase transition in the large  $N$  limit at a temperature below the Hagedorn temperature  $T = T_s$ [21]. This phase transition was identified with the Horowitz-Polchinski correspondence point[22] when the size of UB becomes comparable to string scale ( $r_u \sim l_s$ )[23]. Even for the weakly coupled system, the phase transition is similar to the strongly coupled case[24].

From the microcanonical analysis, it is known that the d=10 Schwarzschild black hole plays an important role at the Hagedorn transition [25, 24]. The canonical instability of the d=10 Schwarzschild black hole is well known on account of its negative heat capacity. A gas of thermal gravitons is also unstable to gravitational collapse due to Jeans instability. Both processes cannot end in a large, stable black hole (sbh) without introducing a cavity. Actually, the d=10 Hagedorn regime is bounded by d=10 black hole and graviton phases[7, 9, 10]. For the large 't Hooft coupling  $\lambda^{1/4}$ , the density of states of type IIB string theory on AdS<sub>5</sub>  $\times$   $S^5$  has four distinct regimes<sup>1</sup>. All phases of gravitons, strings, and black holes dominated by localized degrees of freedom in d=10 disappear, since we are working with the canonical ensemble. However, introducing a confining cavity with size  $R$  as the IR regulator, we have a stable canonical ensemble to study the Hagedorn transition. Then it is possible to connect the tachyon instability to the instability of the d=10 black hole that ends in a sbh.

In this work, we will describe the process of tachyon condensation by using the off-shell gravity/gauge correspondence. For this purpose, we use the off-shell free energy on the bulk/boundary sides. Since we have a hot temperature of  $T = T_s$  in the decay of the superheated Hagedorn states, the endpoint is the plasma state of a radiated CFT (SB). On the gravity-side, this corresponds to a SBH. Further, we use the d=10 Schwarzschild black hole in a cavity to investigate the tachyon instability.

The organization of this work is as follows. Section 2 is devoted to studying the Hawking-Page phase transition for the nucleation of a black hole. The on/off-shell free

---

<sup>1</sup>The AdS/CFT dictionary shows  $\lambda = g_{YM}^2 N$ ,  $g_{YM}^2 = 4\pi g_s$ , and  $l = \lambda^{1/4} l_s$  with  $l$  the AdS-curvature radius and radius of  $S^5$ .  $S \sim E^{9/10}$  for d=10 gravitons with  $E \ll \lambda^{1/4}$ ;  $S \sim E$  for d=10 strings with  $E \gg \lambda^{5/2}$ ;  $S \sim E^{8/7}$ , d=10 black hole with  $E \gg N^2/\lambda^{7/4}$ ;  $S \sim E^{3/4}$  for AdS<sub>5</sub> black hole and its CFT dual with  $E > N^2$ [24].

energies are used to show how the phase transition occurs. The Cardy-Verlinde formula is introduced to define the  $\mathcal{C}_{BH}$ -function. In section 3, we investigate how the Hagedorn transition could be used to describe the process of quasilocal tachyon condensation. We use the off-shell free energy and  $\beta_{BH}$ -function to investigate the off-shell configurations. Inspired by the AdS/CFT correspondence, in section 4 we introduce the Hawking-Page and Hagedorn transition on the CFT side to study the process of tachyon condensation. In section 5, we propose the d=10 Schwarzschild black hole in a cavity to describe the tachyon condensation at the intermediate energy scale. Finally we summarize our important results in section 6.

## 2 Hawking-Page transition

In this section, we review the phase transition between an AdS black hole and thermal AdS space. We start with the d=5 Schwarzschild-AdS black hole[26, 27, 28, 29, 20]

$$ds_{ADSBH}^2 = -\left[1 + \frac{r^2}{l^2} - \frac{m}{r^2}\right]dt^2 + \frac{dr^2}{1 + \frac{r^2}{l^2} - \frac{m}{r^2}} + r^2 d\Omega_3. \quad (1)$$

Here the reduced mass  $m = r_+^2(1 + r_+^2/l^2)$  is determined by the horizon radius  $r_+^2 = (l^2/2)[-1 + \sqrt{1 + 4m/l^2}]$ . The ADM mass  $M = E_{BH}^A$  is related to the reduced mass  $m$  as  $M = \frac{3V_3 m}{16\pi G_5}$  with  $V_3 = 2\pi^2$  the volume of unit three sphere. It possesses a continuous mass spectrum from  $M(l, r_+)$  to thermal AdS with  $M(l, 0) = 0$ :

$$ds_{ADS}^2 = -(1 + r^2/l^2)dt^2 + (1 + r^2/l^2)^{-1}dr^2 + r^2 d\Omega_3^2. \quad (2)$$

Its Hawking temperature and heat capacity are given by[30]

$$T_H^A(l, r_+) = \frac{1}{2\pi} \left[ \frac{1}{r_+} + \frac{2r_+}{l^2} \right], \quad C_{BH}^A(l, r_+) = \frac{3V_3 r_+^2}{2G_5} \left[ \frac{r_+^2 + r_0^2}{r_+^2 - r_0^2} \right] \quad (3)$$

with  $r_0 = l/\sqrt{2}$ .  $T_H^A$  has the minimum value of [15]

$$T_0 = \frac{\sqrt{2}}{\pi l} \quad (4)$$

at the minimum length  $r_+ = r_0$ , and grows linearly for large  $r_+$  due to the presence of a negative cosmological constant  $\Lambda = -6/l^2$ . A solution to the thermal equilibrium (on-shell) condition of  $T_H^A = T$  corresponds to small, unstable black hole (UBH) with radius  $r_u = (\pi l^2 T/2)[1 - \sqrt{1 - 8/(2\pi l T)^2}] \leq r_0$ , while one is large, stable black hole (SBH) with radius  $r_s = (\pi l^2 T/2)[1 + \sqrt{1 - 8/(2\pi l T)^2}] \geq r_0$ . Here we find an inequality of the

temperature  $T \geq T_0$  and a sequence of  $r_u < r_0 = 35 < r_s$  for  $l = 50$ . For  $T \gg 1/l$ , we have approximate on-shell relations of  $r_u \simeq 1/2\pi T$  and  $r_s \simeq \pi l^2 T$ . In the off-shell case of  $T \neq T_H^A$ , there is no direct relation between  $r_+$  and  $T$ . In this sense, we may regard  $r_+$  as the effective temperature. For  $T < T_0$ , there is no solution to  $T_H^A = T$ , which means that no black hole can exist in AdS space. The heat capacity in Eq.(3) has an unbounded discontinuity at  $r_+ = r_0$ , signaling a first-order phase transition from negative heat capacity to positive one. However, the heat capacity determines the thermal stability of a system: thermally stable (unstable) if  $C_{BH}^A > 0$  ( $C_{BH}^A < 0$ ). We get an important piece of information from the study of the BH-free energy

$$F_{BH}^{on}(l, r_+) = E_{BH}^A - T_H^A S_{BH}^A \equiv F_{UBH}^{on} + F_{SBH}^{on}, \quad (5)$$

where

$$S_{BH}^A = \frac{V_3}{4G_5} r_+^3, \quad F_{UBH}^{on} = \frac{V_3 r_+^2}{16\pi G_5}, \quad F_{SBH}^{on} = -\hat{r}^2 F_{UBH}^{on} \quad (6)$$

with  $\hat{r} = r_+/l$ . This applies to saddle points of  $r_u$  and  $r_s$  only. We observe a change of sign between  $F_{BH}^{on}(l, r_+ \ll l) \simeq F_{UBH}^{on} \sim r_+^2$  and  $F_{BH}^{on}(l, r_+ \gg l) \simeq F_{SBH}^{on} \sim -r_+^4$ . This shows that an UBH is unstable to decay into thermal AdS space, while a SBH is stable against decay. For  $r_+ \gg l$ , we have an approximate entropy-energy relation of  $S_{BH}^A \sim (E_{BH}^A)^{3/4}$ , which means that a large black hole has a stable canonical ensemble. Here we have the transition point of  $r_+ = r_1 = l$  from  $F_{BH}^{on}(l, r_+) = 0$ . Plugging this into Eq.(3) leads to the transition temperature[15, 26, 27, 28, 29]

$$T_1 = \frac{3}{2\pi l} \quad (7)$$

which is the critical temperature for the Hawking-Page phase transition.

Assuming the CFT-dual, we introduce the Casimir energy for the black hole<sup>2</sup> [31]

$$E_{BH}^c \equiv 4E_{BH}^A - 3T_H^A S_{BH}^A = \frac{3V_3 r_+^2}{8\pi G_5}. \quad (8)$$

It allows us to write the Cardy-Verlinde formula on the bulk-side[32]

$$S_{BH}^A = \frac{2\pi l}{3} \sqrt{E_{BH}^c (2E_{BH}^A - E_{BH}^c)}. \quad (9)$$

This is an exact relation between entropy and energy. Minimization with respect to  $E_{BH}^c$  leads to the bound  $S_{BH}^A \leq (1/T_1) E_{BH}^A$ , which is called the AdS-Bekenstein bound. This

---

<sup>2</sup>Frankly, it is hard to define the bulk-Casimir energy unless assuming the presence of its dual CFT. Hence it is fairly asserted that the Cardy-Verlinde formula in Eq. (9) on the bulk-side comes from its Cardy-Verlinde formula in Eq. (33) on the boundary.

is not only the upper bound for  $S_{BH}^A$ , but the lower bound for  $E_{BH}^A$ . The saturation of this bound is achieved at the transition point  $r_+ = r_1$ . Here we have thermal relations:

$$E_{BH}^A = E_{BH}^c = S_{BH}^A = 0, \quad F_{BH}^{on} > 0, \quad \text{for } r_+ < r_1 \quad (10)$$

$$E_{BH}^A = E_{BH}^c = T_1 S_{BH}^A, \quad F_{BH}^{on} = 0, \quad \text{for } r_+ = r_1 \quad (11)$$

$$E_{BH}^A > E_{BH}^c, \quad S_{BH}^A < (1/T_1) E_{BH}^A, \quad F_{BH}^{on} < 0, \quad \text{for } r_+ > r_1. \quad (12)$$

This means that the Cardy-Verlinde formula is valid only for on-shell with  $r_+ \geq r_1$ , that is, for a SBH.

Further, defining the Casimir entropy as  $S_{BH}^c = E_{BH}^c/T_1 = V_3 l r_+^2/4G_5$ , the BH-free energy takes the form

$$lF_{BH}^{on} = \frac{S_{BH}^c}{4\pi} [1 - \hat{r}^2]. \quad (13)$$

If  $\hat{r} \rightarrow \delta^{-1}$ , this is analogous to the d=2 free energy of  $lF_2 = \frac{c}{24}(1 - \delta^{-2})$  for  $c$  free bosons. Here we find a relation  $c = 6S_2/\pi$  between the central charge  $c$  and the Casimir entropy  $S_2$  in CFT<sub>2</sub>. In this work we choose a slightly different notation to go together with its dual CFT. The  $\mathcal{C}_{BH}$ -function is defined as

$$\mathcal{C}_{BH}(l, r_+) \equiv \frac{S_{BH}^c}{4\pi} = \frac{V_3 l r_+^2}{16\pi G_5}, \quad r_+ \geq r_1 \quad (14)$$

which is useful for describing the bulk RG-flow in the Hagedorn transition. From Eq.(10), one finds  $\mathcal{C}_{BH}(l, r_+) = 0$ , for  $0 \leq r_+ < r_1$ .

In order to discuss the phase transition more explicitly, we introduce the generalized free energy  $F_{BH}^{off} = E_{BH}^A - T S_{BH}^A$ , which applies to any value of  $r_+$  with the fixed  $T$ [16, 9, 10]. It is given by

$$F_{BH}^{off}(l, r_+, T) = F_{UBH}^{off} + F_{SBH}^{off}, \quad (15)$$

where

$$F_{UBH}^{off} = 3F_{UBH}^{on} \left[1 - \frac{2}{3} \frac{T}{T_H^A}\right], \quad F_{SBH}^{off} = -3F_{SBH}^{on} \left[1 - \frac{4}{3} \frac{T}{T_H^A}\right] \quad (16)$$

Its connection to the action is given by  $I_{BH} = \beta F_{BH}^{off}$ . In case of  $r_+ \ll l$  ( $\hat{r} \ll 1$ ), we approximate  $F_{BH}^{off}$  by  $F_{UBH}^{off}$ , while for  $r_+ \gg l$  ( $\hat{r} \gg 1$ ), it is approximated to be  $F_{SBH}^{off}$ . As is shown in Fig. 1, for  $T = T_0$ , an extremum appears at  $r_+ = r_0 (= r_u = r_s)$ . We confirm that for  $T > T_0$ , there are two saddle points, UBH with radius  $r_u$  and SBH with radius  $r_s$ .  $F_{BH}^{on}$  is composed of a set of two saddle points for  $F_{BH}^{off}$ . That is,  $F_{BH}^{on}$  can be obtained from  $F_{BH}^{off}$  through the operation:  $\partial F_{BH}^{off}/\partial r_+ = 0 \rightarrow T = T_H^A \rightarrow F_{BH}^{off} = F_{BH}^{off}$ . Hence the BH-free energy  $F_{BH}^{on}$  is regarded as the on-shell (equilibrium) free energy, whereas the generalized free energy  $F_{BH}^{off}$  corresponds to the off-shell (non-equilibrium) free energy.

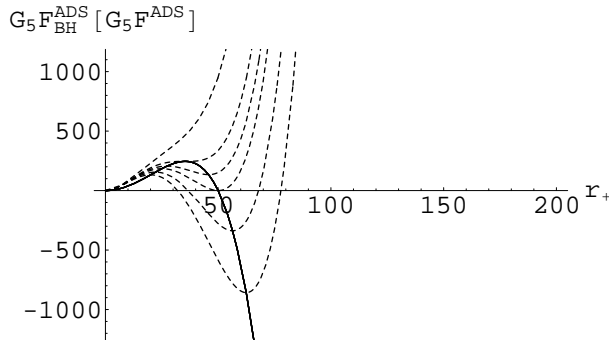


Figure 1: The process of black hole nucleation as in the Hawking-Page phase transition. Here  $r_+$  plays a role of the effective temperature for the BH-free energy, but it is merely a coordinate for the generalized free energy with the fixed  $T$ . The solid line represents the BH-free energy  $F_{BH}^{gn}(l=50, r_+)$  in the units of  $G_5$ , while the dashed line denotes the generalized free energy  $F_{BH}^{off}(l=50, r_+, T)$  for six different temperatures: from the top to bottom,  $T = 0.008, T_0(= 0.009), 0.0093, T_1(= 0.0095), 0.01, 0.0105$ .

All saddle points including thermal AdS at  $r_+ = 0$  contribute dominantly to the path integral evaluation for canonical ensemble.

At this stage, we briefly describe the Hawking-Page transition[15]. For  $T_0 < T < T_1$ , we have a sequence (see the third dashed graph in Fig. 1)

$$F_{BH}^{off}(r_+ = 0) = 0 < F_{BH}^{off}(r_+ = r_s) < F_{BH}^{off}(r_+ = r_u) \quad (17)$$

which means that the saddle point for thermal AdS dominates. For  $T > T_1$ , the SBH dominates because of  $F_{BH}^{off}(r_+ = r_s) < 0$ . There is a change of dominance at the critical temperature  $T = T_1$ . The UBH plays a role of the mediator for the transition between thermal AdS and SBH. In case of  $T < T_1$ , the system is described by a thermal gas, whereas above  $T_1$  it is described by a SBH. This is the Hawking-Page transition for black hole nucleation.

Finally, we introduce the classical gravitational effect of thermal radiation in AdS space. From a relation of  $T_2^5 r_+^4 \sim r_+^4 / G_5 l^2$  for  $r_+ \gg l$ , we find the collapsing temperature  $T_2 = 1 / (G_5 l^2)^{1/5}$ . Thermal radiation at  $T > T_2$  would not be able to support itself against its self-gravity and thus it would collapse to form a black hole. The collapsing temperature of  $T_2 > T_s$  is much greater than  $T_0$  and  $T_1$  because of  $(G_5 l^2)^{1/5} \sim l / N^{2/5} < 1$ . Hence, in this work, we exclude the gravitational collapse of thermal AdS from our consideration.

### 3 Hagedorn transition and quasilocal tachyon condensation

We start with the Hagedorn transition in the type IIB string theory on  $\text{AdS}_5 \times S^5$ . A good model for the Hagedorn spectrum is to consider the highly excited strings as a random walk. Its microcanonical density of states takes the form

$$\Omega(E) = \exp(\beta_s E + \dots), \quad (18)$$

where the ellipsis is  $c\sqrt{E}(-c'E^{16}e^{-\eta E})$  for open strings (closed strings).

According to the AdS/CFT correspondence, Witten has shown that a SBH in AdS space could be described by the deconfinement phase of  $\mathcal{N} = 4$  SYM theory on  $S^1 \times S^3$ . Further, the Hawking-Page transition corresponds to a large  $N$  deconfinement transition in the strongly coupled gauge theory. At strong coupling, the Hagedorn temperature  $T = T_s = 1$  is much greater than the critical temperature  $T_1 = 3/2\pi l$  for the Hawking-Page transition. According to Hagedorn censorship, it was proposed that the regime of Hagedorn transition cannot be studied in terms of the Hawking-Page transition. This is because although the Hagedorn phase is stable microcanonically, but it is unstable canonically. Once the temperature reaches the Hagedorn temperature, the hotter heat reservoir pumps energy into the system until it reaches a large, stable AdS black hole.

However, we use this property to describe the Hagedorn tachyon condensation. For this purpose, we use the winding tachyonic modes from a warped Scherk-Schwarz compactification with topology  $S^1 \times Y$ . The winding tachyon instability causes the circle  $S^1$  on the cone to pinch off when the size of  $S^1$  reaches the string scale  $l_s$ , removing the cone of large curvature sector  $X$  from the small cone including the singularity. We are interested in the evolution of the tachyon instability in the former sector  $X$ , although the latter can be used to study the singularity and unitarity issues in the stringy black hole by using the tachyon condensate phase. The former process is related to the formation and growth of an off-shell black hole with its near horizon geometry ( $<$ ), while the latter process is considered as the formation and evaporation of an off-shell black hole with its shape ( $<>$ ) on the gravity side. If the singularity is replaced by the tachyon phase[12, 13], its shape is given by  $|T \rangle$ . If the dilaton could be kept small throughout the background  $X$ , the process of the closed-string tachyon condensation can be viewed either some RG-flow on the world sheet or off-shell bulk/boundary flows. Let us introduce the AdS regularization for a string gas in  $\text{AdS}_5 \times S^5$  of type IIB string theory, whose metric is given by

$$ds_{10\text{ADS}}^2 = ds_{\text{ADS}}^2 + l^2 d\Omega_5^2 \quad (19)$$



where  $l = \lambda^{1/4}$ <sup>3</sup> with  $N$  the quantum number of Ramond-Ramond flux on  $S^5$ . The time circle in thermal AdS<sub>5</sub> is non-contractible and thus the winding number is preserved. Hence we propose that the stringy geometry resulting from the off-shell tachyon dynamics with  $\sigma \sim m_s r_c$  matches onto the off-shell AdS black hole with the horizon radius  $r_+ \sim r_{st} \in \{l_s, l\}$ . Here  $\sigma$  is an effective tachyon,  $m_s = 1/l_s$  is the mass of string, and  $r_c$  is a capping radius.  $X_{st}$  is introduced to denote the corresponding Euclidean geometry with a conical singularity at the event horizon. Hence its near horizon geometry takes a shape of “<”. Then the process of the off-shell black hole growth provides a good way to escape from the Hagedorn regime of  $0 \leq r_+ \leq l$ . That is, the off-shell black hole continues to grow until it arrives at a SBH with  $r_+ = r_s$ . The endpoint geometry  $X_s$  is the Euclidean section of the AdS black hole with metric

$$ds_{10ADSBH}^2 = ds_{ADSBH}^2 + l^2 d\Omega_5^2. \quad (20)$$

The on-shell manifold  $X_s$  has topology of  $R^2 \times S^3 \times S^5$ , which is considered as a capping of  $X_c$  at  $r_+ = r_s$  [7, 9, 10]. Here  $X_c$  corresponds to the Euclidean off-shell black hole with a conical singularity (<). Hence its near horizon geometry takes a shape of “C”, where there is no singularity at the event horizon. The capping is a progressive effect if  $X_c \in (X_{st}, X_s)$ . This is a topology changing process, where we have non-equilibrium configuration  $T \neq T_H^A$ .

At this stage, we introduce the off-shell parameter  $\alpha$  related to the deficit angle  $\delta$  [35]

$$\alpha(l, r_+, T) = \frac{T_H^A(l, r_+)}{T} \equiv 1 - \frac{\delta(l, r_+, T)}{2\pi}. \quad (21)$$

Then the off-shell free energy takes the form

$$F_{BH}^{off}(l, r_+, T) = \frac{F_{BH}^{on}}{\alpha} + \frac{(\alpha - 1)}{\alpha} E_{BH}^A, \quad (22)$$

where the first term is similar to the on-shell free energy, while the second one determines the off-shell nature of the free energy. Here the corresponding action is given by  $I_{BH} = \beta F_{BH}^{off}$ . For  $\alpha = 1$  ( $T = T_H^A$ ,  $\delta = 0$ ), we recover two saddle points which satisfy  $F_{BH}^{off} = F_{BH}^{on}$ . Hence, for fixed  $T \neq T_H^A$ ,  $F_{BH}^{off}$  describes off-shell configurations very well. As is shown in Fig. 2, the off-shell parameter  $\alpha$  behaves like the temperature of a cool (off-shell) black hole but the deficit angle  $\delta$  has the maximum at  $r_+ = r_0$  and decreases to

---

<sup>3</sup> The d=10 Newton constant is given by  $G_{10} = 2^3 \pi^6 g_s^2 l_s^8$  and its relation to the d=5 Newton constant is  $G_{10} = V(S^5) G_5 = \pi^3 l^5 G_5$ . Then  $N^2 = l^8 / (16\pi^2 g_s^2 l_s^8) = \pi l^3 / 2 G_5$  [33, 34]. For a numerical computation, we use string units:  $l_s = \sqrt{\alpha'} = 1$ . A strongly coupled regime is chosen to be  $g_s = \pi > 1$ . For  $l = \lambda^{1/4} = 50$ ,  $N^2 = 2.5 \times 10^{10}$ ,  $G_{10} = 75908$ ,  $G_5 = 7.8 \times 10^{-6}$ ,  $(G_5 l^2)^{1/5} = 0.455 < 1$ . The radius of Jeans instability at string scale is  $r_{st}^J = l_s / g_s = 0.318$ .

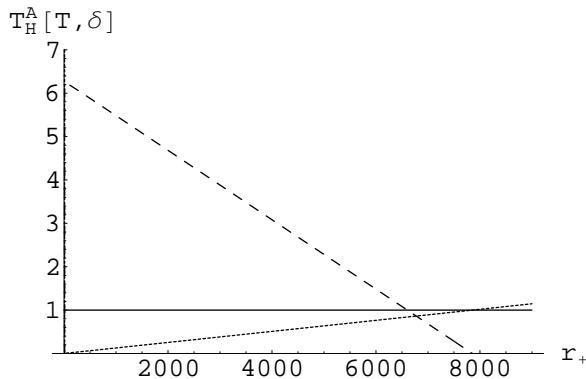


Figure 2: The temperature picture of a cool (off-shell) black hole growth in a hotter heat bath at  $T > T_H^A$ . Solid line: hotter temperature of heat reservoir at Hagedorn temperature  $T = T_s = 1$ . Dotted line: plot of the increasing temperature  $T_H^A$  of a cool black hole with  $l = 50$ . Also, this graph indicates the off-shell parameter  $\alpha(l = 50, r_+, 1)$ . Dashed line denotes the deficit angle  $\delta(l = 50, r_+, 1)$ . In this case we have the sequence of points :  $r_u = 0.159 < r_0 = 35 < r_s = 7853$ . If a matching occurs at  $r_+ = r_{st} \geq l_s$ , the stringy black hole always grows into a SBH at  $r_+ = r_s$ .

zero at  $r_+ = r_s$ .  $\delta(X)$  classifies a conical singularity at the event horizon. For example,  $\delta(X) = 0$  for on-shell configurations of  $X = X_u, X_s$  without any cone ( $\subset$ ), while it has the maximum value  $\delta(X) = 2\pi(1 - T_0) \simeq 2\pi$  for  $X = X_0$  with the narrowest cone ( $\subset$ ). In general, we have  $0 < \delta(X) < 2\pi$ , for the geometry  $X \in (X_u, X_s)$  with a cone ( $\subset$ ).

Our analysis is based on the heat capacity of the black hole. Neglecting quantum tunneling process[26, 27, 28, 29], we have two cases only. i) If the initial black hole state satisfies  $r_+ < r_u$ , there is no black hole state because the black hole evaporates until it arrives at its final state of thermal AdS. ii) If  $r_+ > r_u$  initially, this black hole grows into a SBH with size  $r_+ = r_s$ . Hence, if the stringy black hole is formed with a size  $r_{st} \geq l_s$ , this grows into a globally stable black hole with  $r_s \simeq \pi l^2 T_s = 7853$  by absorbing the remaining string gas in AdS space. This feature is depicted in Fig. 2.

In our picture, the generalized free energy in Eq. (22) can be used to explain this non-equilibrium process. Here we choose the free energy for thermal AdS ( $X_{ADS}$ ) to be zero. Considering  $X_c \in \{X_{st}, X_s\}$ ,  $X_c$  has the conical singularity and its off-shell free energy is given by a point  $F_{BH}^{off}(X_c)$  on the dashed graph in Fig. 3 for  $r_+ \ll l$  and Fig. 4 for  $r_+ \gg l$ . As the initial off-shell black hole ( $F_{BH}^{off}(X_{st})$ ) flows into the final black hole ( $F_{BH}^{off}(X_s)$ ), an off-shell free energy curve ( $F_{BH}^{off}(X_c)$ ) connects  $X_{st}$  to  $X_{bh}$ .

Barbon and Rabinovici[7] assumed that, for  $T \geq T_s$ , the barrier of the UBH is completely washed out by the tree-level string effect. In this case, at  $r_+ = 0$ , one sees the

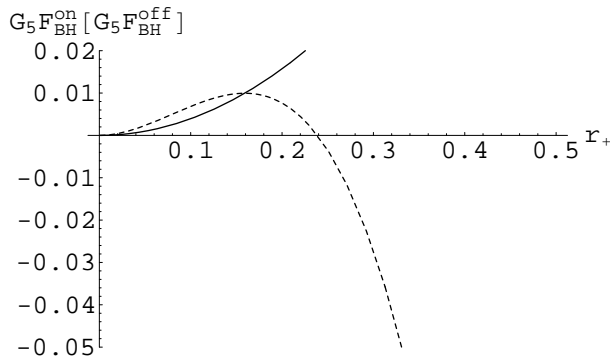


Figure 3: Hagedorn transition with  $T = T_s$  for  $r_+ \ll l$ . The solid line represents the on-shell free energy  $F_{BH}^{on}(50, r_+) \simeq F_{UBH}^{on}(r_+)$ . The dashed line denotes the off-shell free energy  $F_{BH}^{off}(50, r_+, 1) \simeq F_{UBH}^{off}(r_+, 1)$  in the units of  $G_5$ . This picture is described by an UBH. A junction point located at  $r_+ = r_u = 0.159$  is the maximum.

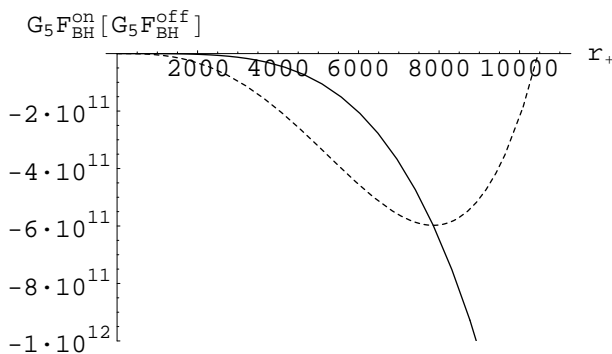


Figure 4: The free energy picture of a cool (off-shell) black hole growth in a hotter heat bath for  $r_+ \gg l = 50$ . The solid line represents the on-shell free energy  $F_{BH}^{on}(50, r_+) \simeq F_{SBH}^{on}(50, r_+) \sim -r_+^4$ , while the dashed lines denote the off-shell free energy  $F_{BH}^{off}(50, r_+, 1) \simeq F_{SBH}^{off}(50, r_+, 1) \sim r_+^4$  in the units of  $G_5$ . A junction point is located at  $r_+ = r_s = 7853$ .

tree-level instability of the Hagedorn tachyon. From Fig. 3, we observe the UBH barrier at  $r_u = 0.159$ , even though its maximum is small as  $G_5 F_{UBH}^{off}(0.159, 1) = 0.009$ . Also we observe the sensitivity around  $r_+ = l_s = 1$  that  $G_5 F_{UBH}^{off}(0.238, 1) = 0$ ,  $G_5 F_{UBH}^{off}(r_{st}^J = 0.318, 1) = -0.039$ ,  $G_5 F_{UBH}^{off}(1, 1) = -3.75$ , and  $G_5 F_{UBH}^{off}(2, 1) = -34.75$ . The distance between the maximum and zero is very small as  $\Delta r_+ = 0.079$ . This shows that the UBH barrier suffers from  $\mathcal{O}(1)$  ambiguity at the Hagedorn temperature. Hence we may take a matching point at  $r_{st} \gg l_s$ . From the relation of  $r_u \simeq 1/2\pi T$ , we conjecture that thermal

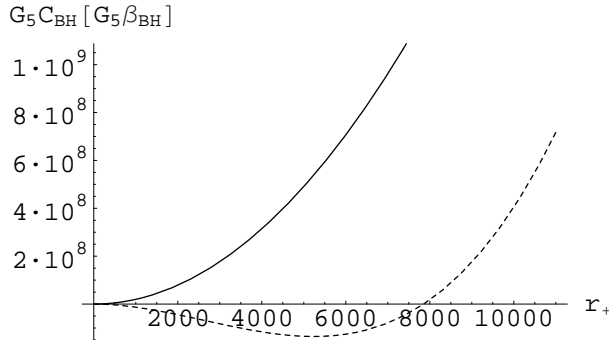


Figure 5: The  $\mathcal{C}_{BH}$  versus  $\beta_{BH}$ -function. The solid line represents the on-shell  $\mathcal{C}_{BH}(50, r_+ \geq r_1)$ -function  $\sim r_+^2$ , while the dashed line denotes the off-shell  $\beta_{BH}(50, r_+, 1)$  in the units of  $G_5$ . The  $\beta_{BH}$ -function is just the derivative of  $F_{BH}^{off}$  with respect to  $r_+$ . Thus it is zero at the saddle points of  $r_+ = r_u, r_s$ .

AdS and UBH will merge for large  $T$ .

Inspired by the action relation of  $I_{BH}(l, r_+ = r_c, T = T_s) \simeq \beta l^9 V_{eff}^t(|\sigma| = m_s r_c)$  with  $r_c$  the capping radius and  $m_s = 1/l_s$  the string mass[7, 9, 10], the effective tachyon potential  $V_{eff}^t$  is given by

$$V_{eff}^t(|\sigma| = r_c) \simeq \frac{F_{BH}^{off}(l = 50, r_+ = r_c, T = 1)}{l^9}. \quad (23)$$

The corresponding graph of  $V_{eff}^t$  appears in Fig. 3 for small  $r_+ \ll l$ . For large  $r_+ \gg 1$ , see Fig. 4. This is an approximation to the Atick-Witten effective potential for the thermal tachyon on  $S^1 \times R^9$ [36].

As is shown in Fig. 4, at  $r_+ = r_s = 7853$ , the endpoint of Hagedorn tachyon condensation is a globally stable black hole state in AdS space. The monotonic property of  $\mathcal{C}_{BH}$  provides condition

$$T_H^A \frac{d\mathcal{C}_{BH}(50, r_+)}{dT_H^A} \geq 0 \rightarrow r_+ \geq r_0, \quad (24)$$

which coincides with the positive heat capacity of  $C_{BH}^A \geq 0$ . Combining it with Eq. (14) leads to the monotonicity:  $\Delta\mathcal{C}_{BH}(l, r_+ \geq r_1) \geq 0$ . This shows that there exists a strong relationship between the monotonicity of  $\mathcal{C}_{BH}$  and the thermal stability of a SBH. In general, the  $\mathcal{C}_{BH}$  is closely related to the central charge on the boundary CFT. From Fig. 4 and 5, we confirm the on-shell monotonicity connection between the increasing  $\mathcal{C}_{BH}(l, r_+)$  ( $\nearrow$ ) and the decreasing  $F^{on}(l, r_+)$  ( $\searrow$ ).

Next, we study the off-shell feature. At fixed temperature we move along the renor-

malization group trajectories. From the definition of the bulk  $\beta$ -function, we have

$$\beta_{BH}(l, r_+, T) \propto \frac{\partial I_{BH}}{\partial r_+} = -\frac{6\mathcal{C}_{BH}(l, r_+)}{l} \delta(l, r_+, T). \quad (25)$$

As is shown in Fig. 5, the bulk  $\beta$ -function does not show a monotonic feature and measures the mass of the conical singularity at the event horizon <sup>4</sup>.

The off-shell free energy  $F_{BH}^{off}(l, r_+, T)$  describes the non-equilibrium configurations between  $r_u$  and  $r_s$ . This is a monotonically decreasing function between on-shell configurations of  $X_u$  and  $X_s$  only. Hence we confirm the off-shell correspondence between the decreasing  $F_{BH}^{off}(l, r_+, T)$  ( $\searrow$ ) and the  $\beta$ -function in the shape of  $\searrow \nearrow$ .

## 4 Confining/deconfining and Hagedorn transitions on the strongly coupled CFT side

In this section, we are interested in the confining/deconfining and Hagedorn transitions for a strongly coupled, large  $N$  gauge theories in the high temperature limit. The d=4 CFT on  $R \times S^3$  near infinity is defined by the Einstein static universe [32]:

$$ds_{ESU}^2 = -d\tau^2 + \rho^2 d\Omega_3^2, \quad (26)$$

where  $\tau$  is a time variable in the boundary theory and  $\rho$  is the radius of three sphere  $S^3$ . Now we can determine the above boundary metric by using the bulk metric in Eq.(1) near infinity as

$$ds_b^2 = \lim_{r \rightarrow \infty} \frac{\rho^2}{r^2} ds_{ADSBH}^2 = -d\tau^2 + \rho^2 d\Omega_3^2 \rightarrow ds_{ESU}^2, \quad \tau = \frac{\rho}{l} t. \quad (27)$$

Using the Euclidean formalism on  $S^1 \times S^3$ , we find bulk-boundary relations [39]:

$$T_{CFT} = \frac{l}{\rho} T_H^A = \frac{1}{2\pi\rho} \left[ 2\hat{r} + \frac{1}{\hat{r}} \right], \quad E_{CFT} = \frac{l}{\rho} E_{BH}^A = \frac{3V_3 \kappa \hat{r}^2}{\rho} [1 + \hat{r}^2] \quad (28)$$

and

$$F_{CFT}^{on} = \frac{l}{\rho} F_{BH}^{on} = \frac{V_3 \kappa \hat{r}^2}{\rho} [1 - \hat{r}^2], \quad S_{CFT} = 4\pi \kappa V_3 \hat{r}^3 = S_{BH} \quad (29)$$

with  $\kappa = l^3/16\pi G_5$ . These are a realization of the holographic principle via the AdS/CFT correspondence. We note that all of CFT's quantities are locally measured in the dual

---

<sup>4</sup>Considering  $I_{BH} = F_{BH}^{on}/T_H^A + I_{cs}$ , we can define the mass  $M_{cs}$  of a conical singularity as  $I_{cs} = 4\pi r_+ M_{cs}$  [37, 38]. Then it is given by  $M_{cs} = \left[ \frac{r_+^2 + l^2}{2r_+^2 + l^2} \right] \frac{\beta_{BH}}{8\pi}$  with  $\beta_{BH} = -\frac{3\pi r_+^2}{4G_5} \delta$ . In case of  $r_+ \gg l$ , we have an approximate relation between the  $\beta$ -function and the mass of the conical singularity:  $M_{cs} \simeq \frac{\beta_{BH}}{16\pi}$ .

CFT, even though the bulk quantities are observed at infinity. Hence the AdS-curvature radius  $l$  disappears and instead the boundary radius  $\rho$  of  $S^3$  appears. We introduce  $F_{CFT}^{on} = F_{ub}^{on} + F_{sb}^{on}$  with  $F_{ub}^{on} = V_3\kappa\hat{r}^2/\rho$  and  $F_{sb}^{on} = -\hat{r}^2F_{ub}^{on}$ . As an example, we have a definite relation of  $V_3\kappa = \pi l^3/8G_5 = N^2/4$  for  $\mathcal{N} = 4, SU(N)$  SYM theory[33, 34]. Then its entropy takes the form of  $S_{SYM} = \pi N^2$  at  $\hat{r} = 1$ .

We call these either the UV/IR scaling transformation in the AdS/CFT correspondence or the Tolman red-shift transformation on the gravity side [40]. The scaling factor of  $\sqrt{-g_\infty^{tt}} = l/\rho$  comes from the fact the Killing vector  $\partial/\partial t$  is normalized so that near infinity

$$g\left(\frac{\partial}{\partial t}, \frac{\partial}{\partial t}\right) \rightarrow -\frac{\rho^2}{l^2}. \quad (30)$$

This fixes the red-shifted CFT of  $T_{CFT}$ ,  $E_{CFT}$  and  $F_{CFT}^{on}$ , but the entropy remains unchanged under the UV/IR transformation. On the CFT side, we find the minimum temperature  $T_{CFT}^0 = \sqrt{2}/\pi\rho$  at  $\hat{r} = \hat{r}_0 = 1/\sqrt{2}$  and the critical temperature  $T_{CFT}^1 = 3/2\pi\rho$  from  $F_{CFT}^{on} = 0$  at  $\hat{r} = \hat{r}_1 = 1$  with  $\rho = 1$ . These are useful for describing the confining/deconfining transition on the boundary. There exists a phase transition from bubble to a radiation-like matter on the boundary, as contrasted with the Hawking-Page transition in the bulk. Also we have an approximate relation between entropy and energy:  $S_{CFT} \sim (E_{CFT})^{3/4}$  which is the same form as in the large AdS<sub>5</sub> black hole.

From the thermal equilibrium condition of  $T = T_{CFT}$ , we find two roots of unstable bounce (UB) and stable bounce (SB):

$$\hat{r}_u = \pi\rho T - \sqrt{(\pi\rho T)^2 - 2}, \quad \hat{r}_s = \pi\rho T + \sqrt{(\pi\rho T)^2 - 2}. \quad (31)$$

For  $T \gg 1/\pi\rho$ , we have the limiting forms of  $\hat{r}_u \rightarrow 0$  and  $\hat{r}_s \rightarrow 2\pi\rho T$ . At  $T = T_{CFT}^0$ , we find an extremum at  $\hat{r} = \hat{r}_0 (= \hat{r}_u = \hat{r}_s)$ . For  $T > T_{CFT}^0$ , string theory backgrounds of a bubble at  $\hat{r} = 0$ , UB and SB appear as saddle points in the Euclidean path integral of Yang-Mills theory[23]. The Euclidean UB undergoes the Gross-Witten phase transition in the large  $N$  limit at a temperature below the Hagedorn temperature. This phase transition is identified with the Horowitz-Polchinski correspondence point where the size of UB becomes comparable to string scale ( $\hat{r}_u \sim l_s/l$ ).

For  $\hat{r} > 1$  (high temperature limit of  $\mathcal{N} = 4$  SYM theory), from Eqs.(28) and (29), we have the well-known form for on-shell free energy

$$\rho F_{CFT}^{on,high} \simeq \frac{N^2}{4} \left[ -(\pi\rho T_{CFT})^4 + (\pi\rho T_{CFT})^2 \right]. \quad (32)$$

The Gibbs free energy is defined by  $G_{CFT} = F_{CFT}^{on} + p_{CFT}V = 2V_3\kappa\hat{r}^2/\rho$  with the equation of state  $p_{CFT} = E_{CFT}/3V$  and the volume of the boundary system  $V = V_3\rho^3$ . Then the

Casimir energy is given by  $E_c = 3G_{CFT}$ , which is also given by  $E_c = (l/\rho)E_{BH}^c$ . This shows a feature of thermal CFT defined on the compact manifold  $S^3$ . Now we obtain the Cardy-Verlinde formula instead of  $S_{CFT} \sim (E_{CFT})^{3/4}$ [31]

$$S_{CFT} = \frac{2\pi\rho}{3} \sqrt{E_c(2E_{CFT} - E_c)} \quad (33)$$

which indicates the exact relation between the entropy and energy. Since  $G_{CFT} = E_c/3 = S_c/2\pi\rho$ , we obtain  $c_{CFT} = S_c/4\pi = V_3\kappa\hat{r}^2$  as a generalized central charge at the boundary CFT. We recover the central charge for large  $N$ ,  $\mathcal{N} = 4$  SYM theory

$$c_{SYM} = \frac{N^2}{4} \quad (34)$$

at the confining/deconfining transition point of  $\hat{r} = 1(r_+ = l)$ . The exact form is given by  $c_{CFT} = (N^2 - 1)/4$ . Considering the confining/deconfining transition at the critical temperature  $T = T_{CFT}^1(\hat{r} = 1)$ , we observe the changes of boundary quantities:

$$E_{CFT} = E_c = S_{CFT} = 0, \quad F_{CFT}^{on} > 0, \quad \text{for } \hat{r} < 1 \quad (35)$$

$$E_{CFT} = E_c = T_{CFT}^1 S_{CFT}, \quad F_{CFT}^{on} = 0, \quad \text{for } \hat{r} = 1 \quad (36)$$

$$E_{CFT} > E_c, \quad S_{CFT} < (1/T_{CFT}^1)E_{CFT}, \quad F_{CFT}^{on} < 0, \quad \text{for } \hat{r} > 1. \quad (37)$$

From the above, we confirm that the Bekenstein bound of  $S_{CFT} \leq (1/T_{CFT}^1)E_{CFT}$  is always satisfied with the large  $N$ , SYM theory[41]. Here we note that the Cardy-Verlinde formula is suitable for only the SB. The central charge satisfies the following condition:  $c_{CFT} = 0$ , for  $\hat{r} < 1$ ;  $c_{CFT} = c_{SYM}$ , for  $\hat{r} = 1$ ;  $c_{CFT} = c_{SYM}\hat{r}^2$ , for  $\hat{r} > 1$ . Hence we argue that for  $\hat{r} \geq 1$ , the central charge is a monotonically increasing function of  $\hat{r}$ . Comparing this with the  $\mathcal{C}_{BH}$ -function on the bulk-side, we confirm the on-shell gravity/gauge duality.

In order to describe the Hagedorn transition on the CFT side clearly, we need the off-shell CFT free energy  $F_{CFT}^{off}(\hat{r}, T) = E_{CFT} - TS_{CFT}$  as a function of  $\hat{r}$  and temperature  $T$  of heat reservoir. Its CFT action is given by  $I_{CFT} = \beta F_{CFT}^{off}$ . We find

$$F_{CFT}^{off}(\hat{r}, T) = F_{ub}^{off} + F_{sb}^{off}, \quad (38)$$

where

$$F_{ub}^{off} = 3F_{ub}^{on} \left[ 1 - \frac{2}{3} \frac{T}{T_{CFT}} \right], \quad F_{sb}^{off} = -3F_{sb}^{on} \left[ 1 - \frac{4}{3} \frac{T}{T_{CFT}} \right]. \quad (39)$$

This is identical with that constructed by using the Landau theory of phase transition[42]. Actually,  $F_{CFT}^{off}$  describes the CFT system away from equilibrium ( $T \neq T_{CFT}$ ). We confirm that  $F_{CFT}^{on}$  is the on-shell free energy by using operation:  $\partial F_{CFT}^{off}/\partial\hat{r} = 0 \rightarrow T = T_{CFT} \rightarrow$

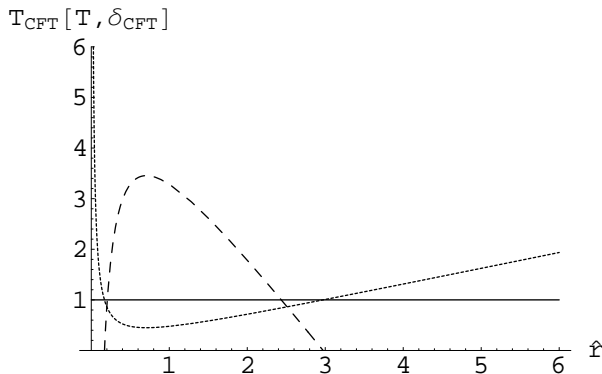


Figure 6: The CFT-temperature picture of the cool (off-shell) bounce growth at the Hagedorn temperature at  $T > T_H$ . Solid line: hotter temperature of heat reservoir at  $T = T_s$  for Hagedorn transition. Dotted line: plot of the CFT temperature  $T_{CFT}(\hat{r}) = \alpha_{CFT}(\hat{r}, 1)$  with  $\rho = 1$ . Dashed line: deficit angle  $\delta_{CFT}(\hat{r}, 1)$ . In this case we have a sequence of temperatures:  $\hat{r}_u = 0.168 < \hat{r}_0 = 0.707 < \hat{r}_s = 2.973$ . If a matching occurs at  $\hat{r}_{st} > \hat{r}_u$ , the off-shell bounce always grows into a SB.

$F_{CFT}^{off} = F_{CFT}^{on}$ . To capture the off-shell feature, we introduce the off-shell parameter  $\alpha_{CFT}$  related the deficit angle  $\delta_{CFT}$

$$\alpha_{CFT}(\hat{r}, T) = \frac{T_{CFT}(\hat{r})}{T} \equiv 1 - \frac{\delta_{CFT}(\hat{r}, T)}{2\pi}. \quad (40)$$

Here the deficit angle takes a value between  $\delta_{CFT}^{min} = 0 (\alpha_{CFT} = 1, T = T_{CFT})$  and  $\delta_{CFT}^{max} = 2(\pi - \sqrt{2})(\hat{r} = \hat{r}_0)$ . See Fig. 6. Then the off-shell free energy takes the form

$$F_{CFT}^{off}(\hat{r}, T) = \frac{F_{CFT}^{on}(\hat{r})}{\alpha_{CFT}} + \frac{(\alpha_{CFT} - 1)}{\alpha_{CFT}} E_{CFT}(\hat{r}), \quad (41)$$

where we check that for  $\alpha_{CFT} = 1$ , we recover  $F_{CFT}^{off} = F_{CFT}^{on}$ . For fixed  $T \neq T_{CFT}$ ,  $F_{CFT}^{off}$  indicates off-shell configurations in the boundary CFT. Hence we expect that in the Hagedorn transition at  $T = T_s > T_1$ , the off-shell free energy  $F_{CFT}^{off}$  describes a process of tachyonic condensation.

In Fig. 7, the solid line represents the on-shell CFT free energy  $F_{CFT}^{on}(\hat{r}) \simeq F_{ub}^{on}(\hat{r})$  with  $\rho = 1$ . The dashed line denotes the off-shell CFT free energy  $F_{CFT}^{off}(\hat{r}, 1) = F_{ub}^{off}(\hat{r}, 1)$ , where the maximum is at  $\hat{r}_u$ . As is shown in Fig. 8, the solid line represents the on-shell free energy  $F_{CFT}^{on}(\hat{r})$  which is the maximum at  $\hat{r} = \hat{r}_0$  and zero at  $\hat{r} = \hat{r}_1 = 1$ . The dashed line denotes the off-shell free energy  $F_{CFT}^{off}(\hat{r}, 1) \simeq F_{sb}^{off}(\hat{r}, T = 1)$  to connect  $\hat{r}_u$  with  $\hat{r}_s$  in the units of  $G_5$ . At  $\hat{r} = \hat{r}_s$ , we have the endpoint of Hagedorn tachyon condensation as a SB. Comparing these with the bulk results, we confirm the gravity/gauge duality.



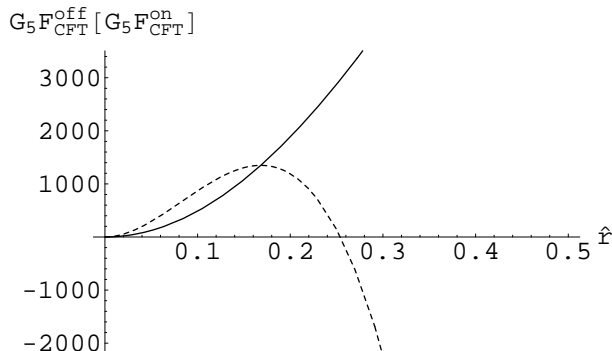


Figure 7: The CFT-free energy picture of cool (off-shell) bounce growth in a heat reservoir at  $T = T_s$  for  $\hat{r} < 1$ .

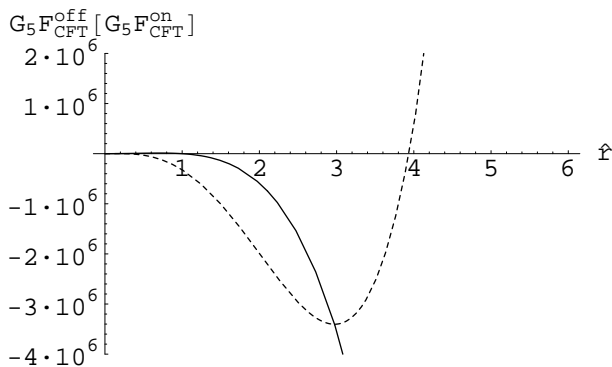


Figure 8: The CFT-free energy picture of cool (off-shell) bounce growth in a heat reservoir at  $T = T_s$ .

In thermodynamics,  $\Delta G_{CFT} \geq 0$  holds for irreversible processes. Similarly  $\Delta c_{CFT} \geq 0$  shows a thermodynamic Zamolodchikov's theorem. As is shown Fig. 9, the central charge function  $c_{CFT}(\hat{r} \geq 1)$  is a monotonically increasing function ( $\nearrow$ ). The on-shell free energy  $F_{CFT}^{on}(\hat{r})$  is a monotonically decreasing function ( $\searrow$ ). Hence we have a monotonicity between  $c_{CFT}(\hat{r})$  with  $\nearrow$  and  $F^{on}(\hat{r})$  with  $\searrow$ .

Now we discuss the off-shell picture. From the definition of the CFT  $\beta$ -function, we have

$$\beta_{CFT}(\hat{r}, T) \propto \frac{\partial I_{CFT}}{\partial \hat{r}} = -6c_{CFT}(\hat{r})\delta_{CFT}(\hat{r}, T). \quad (42)$$

As is shown in Fig. 9, this CFT  $\beta$ -function (holographic RG-flow) is similar to the  $\beta$ -function on the world sheet (RG-flow). Thus the holographic RG-flow is just an irreversible thermal process in the boundary thermal CFT. On the other hand, the off-shell free energy  $F_{CFT}^{off}(\hat{r}, 1)$  is a monotonically decreasing function, which is responsible for the

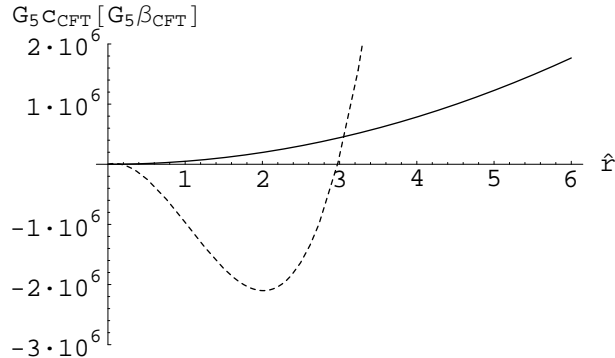


Figure 9: The central charge function  $c_{CFT}(\hat{r})$  and the CFT  $\beta$ -function. The solid line represents the (on-shell) central charge  $c_{CFT}(\hat{r} \geq 1)$  which is a monotonically increasing function, while the dashed line denotes the off-shell  $\beta_{CFT}(\hat{r}, 1)$ . The latter is zero when  $\delta_{CFT} = 0$ .

off-shell bounce growth. Hence we confirm the off-shell connection between  $F_{CFT}^{off}(\hat{r}, 1)$  with  $\searrow$  and  $\beta_{CFT}(\hat{r}, 1)$  in the shape of  $\searrow \nearrow$ .

Finally, we comment on the similarity and difference between the bulk quantities in sections 2 and 3, and the boundary quantities in this section. First we observe a close similarity between two systems from Eqs. (28) and (29). It is obvious from the holographic principle that there exist bulk-boundary relations for thermodynamic quantities. Therefore, we observe the similarity between Figs. 3, 4, 5 and Figs. 7, 8, 9. However, we find crucial differences. First of all, we could not define the black hole pressure (presumably,  $p_{BH} = 0$ ), while the pressure of the CFT is  $p_{CFT} = \rho_{CFT}/3$  in the high temperature limit of  $\mathcal{N} = 4$  SYM theory. That is, the CFT plays a role of the radiation-like matter. This means that we may read off the pressure of the black hole from its dual CFT. The Cardy-Verlinde formula in Eq. (33) was originally defined for the gauge theory of CFT on the boundary [32]. As an analogy, we define the Cardy-Verlinde formula in Eq. (9) on the bulk-side. Hence the meaning of the central charge  $c_{CFT}$  is more clear than that of  $\mathcal{C}_{BH}$ -function. The former shows the number of degrees of freedom, while the latter is just a function related to the heat capacity of the black hole. In addition, the  $F_{BH}^{off}$  and  $\beta_{BH}$  describes the growth of a black hole with the conical singularity at the horizon, while  $F_{CFT}^{off}$  and  $\beta_{CFT}$  describe the growth of the bounce on the boundary.

## 5 d=10 Schwarzschild black hole in a cavity

Now we study the tachyon condensation in the d=10 Schwarzschild black hole (bh)[7]. Here we achieve the IR regularization by introducing a confining cavity instead of AdS regularization<sup>5</sup>. Then we may connect the d=10 Hagedorn strings to a black hole instability that ends in the large, stable black hole.

We start with the d=10 Schwarzschild black hole spacetime

$$ds_{10Sch}^2 = -\left[1 - \left(\frac{r_+}{r}\right)^7\right]dt^2 + \frac{dr^2}{1 - \left(\frac{r_+}{r}\right)^7} + r^2 d\Omega_8^2 \quad (43)$$

whose thermodynamic quantities as measured at infinity are given by

$$E^\infty = M = \frac{V_8 r_+^7}{2\pi G_{10}}, \quad T_H^\infty = \frac{7}{4\pi r_+}, \quad C_{bh}^\infty = -\frac{2V_8 r_+^8}{G_{10}} \quad (44)$$

with the volume of the unit eight sphere  $V_8 = 32\pi^4/105$  and the d=10 Newton constant  $G_{10}$ . The bh-free energy and generalized free energy are

$$F_{bh}^\infty = \frac{V_8 r_+^7}{16\pi G_{10}}, \quad F^\infty = E^\infty - T \cdot S_{bh} = M\left[1 - \frac{7}{8} \frac{T}{T_H^\infty}\right], \quad S_{bh} = \frac{V_8 r_+^8}{4G_{10}}. \quad (45)$$

It is obvious from Eqs.(44) and (45) that the d=10 Schwarzschild black hole is unstable to decay into thermal gravitons because  $C_{bh}^\infty < 0$  and  $F_{bh}^\infty > 0$ . Also we have the relation of  $S_{bh} \sim (E^\infty)^{8/7}$ , which signals the presence of an unstable canonical ensemble. Considering  $E_c^\infty = 9E^\infty - 8T_H^\infty \cdot S_{bh} = 2E^\infty$ [31], we have the exact relation between entropy and energy:  $S_{bh} = \frac{2\pi r_+}{8} \sqrt{2E^\infty E_c^\infty}$ . Comparing this with Eq.(9) leads to the conclusion that the Schwarzschild black hole is unstable. This black hole can be rendered thermodynamically stable by confining it within a finite ideal isothermal cavity. We assume that a black hole is located at the center of the cavity. Here we fix the temperature  $T$  on its isothermal boundary of radius  $R$ . In an equilibrium configuration, the Hawking temperature measured on the boundary must be equal to the boundary temperature  $T$ [16]

$$T_H(R, r_+) \equiv \frac{T_H^\infty}{\sqrt{1 - \left(\frac{r_+}{R}\right)^7}} = T. \quad (46)$$

This means that, according to the Tolman law, a local observer at rest will measure a local temperature  $T$  which scales as  $1/\sqrt{-g_{00}}$  for any self-gravitating system in thermal

---

<sup>5</sup>The AdS regulator is  $l$ , whereas the d=10 black hole regulator is the radius  $R$  of the cavity.

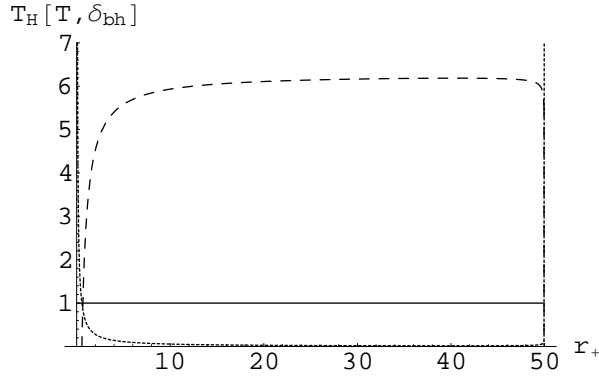


Figure 10: The temperature picture of the d=10 cool (off-shell) black hole growth in a cavity at the Hagedorn temperature at  $T > T_H$ . Dashed line: the deficit angle  $\delta_{bh}(R, r_+, 1)$ . Solid line: hotter temperature of heat reservoir at  $T = T_s$  for Hagedorn transition. Dotted line: the Hawking temperature  $T_H$  of the cold off-shell black hole. In this case we have a sequence of temperatures:  $r_u = 0.557 < r_0 = 40.33 < r_s = 49.99$ . If a matching occurs at  $r_{st} > r_u$ , the stringy black hole always grows into a large, stable black hole at  $r_+ = r_s$ .

equilibrium with heat reservoir. The cavity is the heat reservoir. At  $r_+ = r_0 = (2/9)^{1/7}R$ ,  $T_H$  has the minimum temperature

$$\tilde{T}_0 = \frac{3\sqrt{7}}{4\pi R} \left(\frac{9}{2}\right)^{\frac{1}{7}} \quad (47)$$

which corresponds to the nucleation temperature of a stable black hole. This is depicted in Fig. 10. The equation (46) allows two real, nonzero solutions for a given  $T$ : a smaller unstable black hole (ubh) with radius  $r_u$  and a larger, stable black hole (sbh) with radius  $r_s$ . For  $T < T_0$ , no real value  $r_+$  can solve Eq.(46) and thus no black hole can exist in the cavity. The thermodynamic energy for the black hole embedded in a cavity takes the form of  $E_{bh}(R, r_+) = E^{max} \left(1 - \sqrt{1 - r_+^7/R^7}\right)$  which differs from the ADM mass of  $E^\infty = M$ . Here  $E^{max} = V_8 R^7 / \pi G_{10}$  is the maximum energy of this system when  $r_+ = R$  (system-size black hole). In general, one has  $0 \leq E \leq E^{max}$ . The heat capacity is defined at the constant area  $A$  of the cavity boundary. It is given by  $C_{bh} \equiv (\partial E_{bh} / \partial T_H)_A$  [16]

$$C_{bh}(R, r_+) = C_{bh}^\infty \frac{\left[1 - \left(\frac{r_+}{R}\right)^7\right]}{\left[1 - \frac{9}{2}\left(\frac{r_+}{R}\right)^7\right]}. \quad (48)$$

The bh-free energy of the system is given by  $F_{bh}^{on} = E_{bh} - T_H S_{bh}$ .  $F_{bh} = 0$  leads to  $r_+ = r_1 = (32/81)^{1/7}R$ . Substituting it into Eq.(46), the transition temperature can be obtained as

$$\tilde{T}_1 = \frac{1}{2\pi R} \left[ \left(\frac{9}{2}\right)^{\frac{1}{7}} + 2\left(\frac{2}{9}\right)^{\frac{1}{7}} \right]. \quad (49)$$

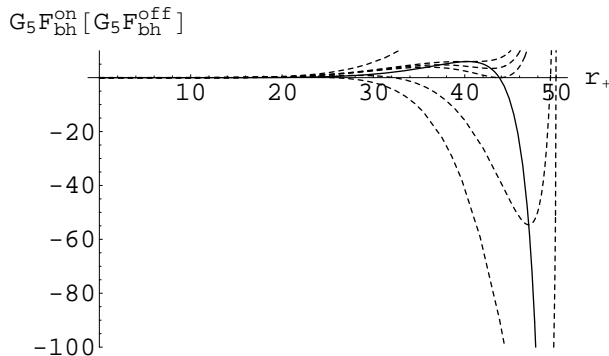


Figure 11: The process of black hole nucleation as the GPY phase transition. The solid line represents the bh-free energy  $F_{bh}^{on}(R = 50, r_+)$ , while the dashed lines denote the generalized free energy  $F_{bh}^{off}(R = 50, r_+, T)$  in the units of  $G_5$ . At  $r_+ = r_0$ ,  $F_{bh}^{on}$  has the maximum value and it is zero at  $r_+ = r_1 = 43.78$ . From the top down, we have the generalized free energy graphs for  $T = 0.01, \tilde{T}_0 (= 0.0156), 0.016, \tilde{T}_1 (= 0.0163), 0.02, 0.025$ .

$C_{bh}$  has an unbounded discontinuity at  $r_+ = r_0 = 40.33$  for  $R = 50$ . Therefore, it seems that the assumed phase transition is first-order at  $T = \tilde{T}_0 = 0.0156$ . However, this behavior of heat capacity in itself does not indicate a phase transition in the canonical ensemble. The heat capacity usually determines thermal stability of the system. Here we find the positive heat capacity for  $r_0 \leq r_+ \leq R$ , indicating stability. On the other hand, the bh-free energy  $F_{bh}^{on}$  has the maximum value at  $r_+ = r_0$  and it becomes zero at  $r_+ = r_1 = 43.78$ . The latter provides  $\tilde{T}_1 = 0.0163$  which is the critical temperature for the GPY phase transition.

To study the GPY and Hagedorn transitions explicitly, we need to introduce the generalized free energy[16, 43]

$$F_{bh}^{off}(R, r_+, T) = E_{bh} - TS_{bh}. \quad (50)$$

The generalized free energy  $F_{bh}^{off}$  plays a role of an effective potential in the canonical ensemble. Here we define the action  $I_{bh} = \beta F_{bh}^{off}$ . The d=10 deficit angle is defined by (see Fig. 10)

$$\delta_{bh}(R, r_+, T) = 2\pi \left[ 1 - \frac{T_H(R, r_+)}{T} \right]. \quad (51)$$

With  $T = \tilde{T}_0$ , an extremum appears at  $r_+ = r_0 (= r_u = r_s)$ . It could be checked by noticing an inflection point in Fig. 11. For  $T > \tilde{T}_0$ , there are two extrema, the ubh with radius  $r_u$  and the sbh with  $r_s$ . We note that for  $\tilde{T}_0 < T < \tilde{T}_1$ ,  $F_{bh}^{off}$  has a saddle point at  $r = r_u$ . This unstable solution is important as the mediator of phase transition from thermal

gravitons to a sbh. In the limit of  $R \rightarrow \infty$ , the sbh is lost and only the ubh survives.  $F_{bh}^{on}$  is a set of saddle points of  $F_{bh}^{off}$ . Now we examine how the tachyon condensation could be realized in this picture[8]. There exists a slight difference in including winding number between AdS and cavity regularization. The Euclidean topology of d=10 Schwarzschild black hole in cavity is  $R^2 \times S^8$ , which is not the cylindrical topology of  $S^1 \times R^9$ . Hence the d=10 Schwarzschild black hole in cavity seems to be unable to include the Hagedorn tachyon condensation, because it does not have a non-contractible circle. Inside the horizon, cylinders with spherical cross sections shrink. Hence it seems that a topologically stable winding tachyon does not appear. Despite this, there may exist a superposition of winding string modes in great circles of  $S^8$ .  $S^8$  starts shrinking rapidly before its spatial curvature becomes large. The change in radius  $r$  with respect to proper time is given by  $\dot{r} = -\sqrt{(r_+/r)^7 - 1}$ , which takes the form of  $-(r_+/r)^{7/2}$  for  $r \ll r_+$ . This means that the velocity  $\dot{r}$  becomes very rapid for  $l_s \ll r \ll r_+$ , while  $S^8$  is still large. Starting from the radius  $r_c$  such that  $(\dot{r}/r)^2|_{r=r_c} = 1/l_s^2$ , one finds a capping radius  $r_c = (r_+^7 l_s^2)^{1/9}$ . This implies that the Hagedorn density of strings is produced by the time the sphere has shrunk to  $r = r_c$ . The backreaction of this string gas may behave like a winding tachyon condensation[44, 45]. When the size of horizon reaches the string scale ( $r_+ \sim l_s$ ), it will pinch off at  $r_c = l_s$ , removing the region of large curvature sector from the small sector including the singularity. This is a process of tachyon condensation in d=10 Schwarzschild black hole. Considering the d=10 Schwarzschild black hole in a cavity, the large sector grows into a sbh (cavity-size black hole).

We discuss the Hagedorn transition by introducing an approximate off-shell free energy to Eq.(50),

$$F_{app}^{off} = 8F_{ubh}^{on} \left[ \left(1 - \frac{7}{8} \frac{T}{T_H}\right) + \frac{1}{4} \left(\frac{r_+}{R}\right)^7 \left(1 - \frac{7}{4} \frac{T}{T_H}\right) \right], \quad F_{ubh}^{on} = \frac{V_8 r_+^7}{2\pi G_{10}} = M \quad (52)$$

which holds for  $r_+ < R$ . In the case of  $r_+ \ll R$ , this leads to the off-shell free energy  $F^\infty$  for the d=10 Schwarzschild back hole. In the case of  $r_+ \sim R$ , the above free energy does not work for the Hagedorn transition because we have to include all higher-order terms of  $(r_+/R)^{7n}$ ,  $n \geq 2$ . However, we find a similarity between Eq.(15) and Eq.(52).

In order to estimate where the ubh and sbh are located, we use Fig. 12 and Fig. 13. From  $F_{BH}^{off}(R = 50, r_+, 1) = F_{bh}^{on}(R = 50, r_+)$ , we obtain the ubh with size  $r_u$  and sbh with size  $r_s \simeq R$ . The latter is a nearly cavity-size black hole. As is shown in Fig. 12, we observe the barrier of the ubh at  $r_u$ , even though its maximum is very small as  $G_5 F^\infty(0.557, 1) = 1.2 \times 10^{-12}$ . Also we observe the sensitivity around  $r_+ = l_s = 1$  that  $G_5 F^\infty(R_{st}^J = 0.318, 1) = 8.9 \times 10^{-14}$ ,  $G_5 F^\infty(0.636, 1) = -13.4 \times 10^{-14}$ ,  $G_5 F^\infty(1, 1) = -2.7 \times 10^{-10}$ , and  $G_5 F^\infty(2, 1) = -1.3 \times 10^{-7}$ . The distance  $\Delta r_+ = 0.079$  between the

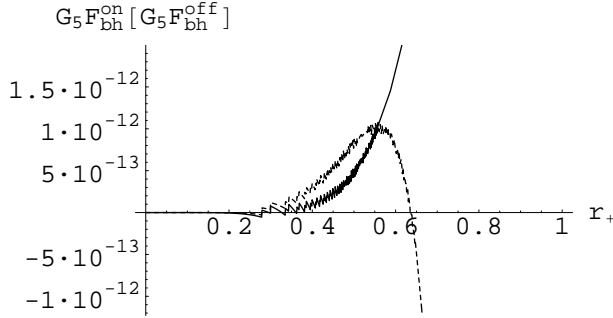


Figure 12: Hagedorn transition with  $T = T_s$  for  $r_+ < 1$ . The solid line represents the bh-free energy  $F_{bh}^{on}(R = 50, r_+) \simeq F_{bh}^\infty(r_+) \sim \mathcal{C}_{bh}(R = 50, r_+)$ , while the dashed line denotes the generalized free energy  $F_{bh}^{off}(50, r_+, 1) \simeq F^\infty(r_+, 1)$ . This picture is described by a small Schwarzschild black hole.

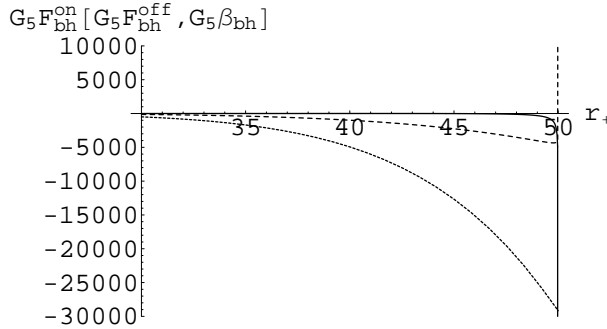


Figure 13: The free energy picture of the d=10 off-shell black hole growth in a cavity at  $T = T_s$  for  $r_+ \gg 1$ . The solid line represents the on-shell free energy  $F_{bh}^{on}(R = 50, r_+)$ , while the dotted line denotes the off-shell free energy  $F_{bh}^{off}(50, r_+, 1)$  in the units of  $G_5$ . The dashed line represents the off-shell  $\beta$ -function  $\beta_{bh}(50, r_+, 1)$ . At  $r_+ = r_s = 49.99$ , we have the endpoint of Hagedorn tachyon condensation as a globally stable black hole state.

maximum and zero is the same as the AdS black hole. Also we observe that the off-shell free energy is very sensitive around the string scale  $r_+ = l_s$ .

We assume that the cavity is filled with thermal gravitons. Considering  $S_{TG} \sim (TR)^9$  and  $RE_{TG} \sim (TR)^{10}$ , one finds the relation of  $S_{TG} \sim (E_{TG})^{9/10}$ . We obtain the collapsing temperature  $T = \tilde{T}_2$  approximately by using the relation

$$E_{TG} = \tilde{T}_2^{10} R^9 \sim E_{bh} \simeq R^7 / G_{10} \quad (53)$$

which shows that  $\tilde{T}_2 \sim 1/(G_{10} R^2)^{1/10}$ . At  $T = \tilde{T}_2 = 0.148$ , the gravitational collapse

of thermal graviton may occur. The collapsing temperature is given by  $\tilde{T}_2 \sim 10\tilde{T}_1$  and the Hagedorn temperature is given by  $T_s \sim 100\tilde{T}_1$ . Hence we are not easy to avoid this collapsing from our consideration, in contrast with the thermal AdS collapse at  $T_2 = 2.195 > T_s$  because of  $\tilde{T}_2 \in (\tilde{T}_1, T_s)$ . It seems that the classical gravitational collapse occurs by the relativistic Jeans instability before the Hagedorn transition at  $T = T_s$ .

Finally, we discuss the connection between the on-shell and off-shell quantities. Since the dual cft to the asymptotically flat d=10 black hole is not yet known, we cannot precisely define the Casimir energy  $E_{bh}^c$  and thus  $\mathcal{C}_{bh}$ . However, assuming  $E_{bh}^c = 2E^\infty$ , we may define  $\mathcal{C}_{bh}(R, r_+) = E_{bh}^c/4\pi\tilde{T}_1 \sim V_8 R r_+^7 / \pi G_{10}$ , which is a monotonically increasing function. Now let us derive the corresponding  $\beta$ -function

$$\beta_{bh}(r_+, T) \propto \frac{\partial I_{bh}}{\partial r_+} \sim -\frac{\mathcal{C}_{bh}(R, r_+)}{R} \delta_{bh}(r_+, T). \quad (54)$$

Hence we have a monotonic connection between  $\mathcal{C}_{bh}(R, r_+)$  with  $\nearrow$  and  $F_{bh}^{on}(R, r_+)$  with  $\searrow$  shown in Fig. 13. Further we confirm the off-shell connection between  $F_{BH}^{off}(R, r_+, 1)$  with  $\searrow$  and  $\beta_{bh}(R, r_+, 1)$  in the shape of  $\searrow\uparrow$ .

## 6 Summary

We study quasilocal tachyon condensation by using the gravity/gauge duality. In order to cure the IR divergence due to tachyon, we introduce two regularization schemes: AdS space and Schwarzschild black hole in a cavity, which provide stable canonical ensembles and thus are good candidates for the endpoint of tachyon condensation. Introducing the Cardy-Verlinde formula, we establish the on-shell gravity/gauge duality. The Cardy-Verlinde formula states exactly the on-shell relationship between the entropy and energy instead of an approximate relation  $S \sim E^{3/4}$  for the AdS black hole and its CFT. We summarize our key results in Table 1. For the tachyon condensation, the on-shell flow is not available. In string theory, the RG  $\beta$ -function shows a collection of off-shell configurations on the world sheet. Further, an effective tachyon potential is given by Eq.(23). First, we note the on-shell correspondence:  $\mathcal{C}_{BH} \rightarrow c_{CFT} \rightarrow \mathcal{C}_{bh}$  for the monotonic increasing  $C$ -function ( $\nearrow$ );  $F_{BH}^{on} \rightarrow F_{CFT}^{on} \rightarrow F_{bh}^{on}$  for the monotonic decreasing free energy  $F^{on}$  ( $\searrow$ ). Then the off-shell correspondence is as follows:  $F_{BH}^{off} \rightarrow F_{CFT}^{off} \rightarrow F_{bh}^{off}$  for the monotonic decreasing free energy  $F^{off}$  ( $\searrow$ );  $\beta_{BH} \rightarrow \beta_{CFT} \rightarrow \beta_{bh}$  for  $\beta$ -function ( $\searrow\uparrow$ ). The connection between these can be found as well. The  $\beta$ -function is the derivative of  $F^{off}$  with respect to  $r_+(\hat{r})$  and measures the mass  $M_{cs} \simeq \beta/16\pi$  of the conical singularity at the event horizon. The on-shell free energy  $F^{on}$  is obtained by substitution of



Table 1: Summary for the Hagedorn transitions at  $T = T_s$  in the study of tachyon condensation. Here is the notation: SP(saddle point), UBH(AdS unstable black hole), SBH(AdS stable black hole), UB(unstable bounce), SB(stable bounce), sbh(d=10 stable black hole), ubh(d=10 unstable black hole), and WST(world sheet topology).

	string theory	AdS-BH	CFT	d=10 bh
on-shell instability	SP(hole)	UBH	UB	ubh
on-shell flow	N/A	$\mathcal{C}_{BH}/F_{BH}^{on}$	$\mathcal{C}_{CFT}/F_{CFT}^{on}$	$\mathcal{C}_{bh}/F_{bh}^{on}$
off-shell matching	tachyon	BH	bounce	bh
off-shell flow	$\beta/V_{eff}^t$	$\beta_{BH}/F_{BH}^{off}$	$\beta_{CFT}/F_{CFT}^{off}$	$\beta_{bh}/F_{bh}^{off}$
off-shell feature	WST change	BH growth	bounce growth	bh growth
on-shell stability	SP(hole)	SBH	SB	sbh

$T \rightarrow T_H^A(T_{CFT}, T_H)$  into  $F^{off}$ . Also this can be seen from the derivative of  $F^{off}$  with respect to  $r_+(\hat{r})$ . The  $C$ -function is proportional to the unstable part  $F_{UBH}^{on}(F_{ub}^{on}, F_{ubh}^{on})$ .

A few of comments are in order. The stringy geometry resulting from the off-shell tachyon dynamics matches onto the off-shell AdS black hole at the matching radius  $r_+ = r_{st} \in \{l_s, l\}$ . In choosing this region, we avoid including the Jeans instability at  $r_{st}^J = 0.318$ , but we take into account the Horowitz-Polchinski correspondence point for black holes and strings at  $r_{HP} \sim l_s$  and the tachyon instability due to the winding number at string scale  $r_+ \sim l_s$ . If the matching occurs at  $r_+ = r_0 = l/\sqrt{2}$ , we find the maximal deficit angle  $\delta(X_0) \simeq 2\pi$ . The amount of free energy released at the moment of the matching is  $F_{BH}^{off}(50, r_+ = r_0, 1) = -215881/G_5 \simeq -10N^2$ . Furthermore, the matching point of  $r_{st} = l_s$  could be extended to  $r_{st} = \mathcal{O}(l)$  unless  $\beta_s - \beta$  is fine-tuned to be very small[7]. For  $r_{st} = l_s$ , the released free energy is given by  $F_{BH}^{off}(50, r_+ = 1, 1) = -35/G_5 \simeq 10^6$ , whereas for  $r_{st} = l$ , the released free energy is  $F_{BH}^{off}(50, r_+ = l, 1) = -610960/G_5 \simeq 30N^2$ . Hence, we confirm that for  $r_{st} \propto \mathcal{O}(l)$ , the released free energy is of order  $N^2$ [9, 10].

Concerning the weakly coupled case, it is known that the phase transition is similar to the strongly coupled case. Of course, the would-be black hole is different from the AdS black hole for the strongly coupled case[24]. Fortunately, the corresponding Cardy-Verlinde formula takes the same form as Eq.(33) replacing  $2\pi\rho/3$  and  $\hat{r} = r_+/l$  by  $4\pi\rho/3$  and  $\delta^{-1} = 2\pi\rho T$  from the free  $\mathcal{N} = 4$  SYM theory[31]. This shows that “2” for  $\lambda^{1/4} \rightarrow \infty$  (in the strong coupling limit), while “4” for  $\lambda^{1/4} \rightarrow 0$  (in the weak coupling limit).

Further, the d=10 Schwarzschild black hole in a cavity is considered a model for the Hagedorn transition which gives a possible explanation of the tachyon condensation. However, it is not clear whether this is truly a model of the tachyon condensation because

of the lack of its dual cft.

In conclusion we explain the process of tachyon condensation by using the off-shell gravity/gauge duality.

## Acknowledgement

The author thanks Steve Hsu and Brian Murray for helpful discussions. This work was supported by the Korea Research Foundation Grant (KRF-2005-013-C00018) and by the Korea Science and Engineering Foundation through the Center for Quantum Spacetime of Sogang University with grant number R11-2005-021.

## References

- [1] A. Dabholkar, Phys. Rev. Lett. **88**, 091301 (2002) [arXiv:hep-th/0111004].
- [2] A. Dabholkar, Nucl. Phys. B **639**, 331 (2002). [arXiv:hep-th/0109019].
- [3] C. Vafa, arXiv:hep-th/0111051.
- [4] Y. Michishita and P. Yi, Phys. Rev. D **65**, 086006 (2002) [arXiv:hep-th/0111199].
- [5] A. Adams, J. Polchinski and E. Silverstein, JHEP **0110**, 029 (2001) [arXiv:hep-th/0108075].
- [6] J. A. Harvey, D. Kutasov, E. J. Martinec and G. W. Moore, arXiv:hep-th/0111154.
- [7] J. L. F. Barbon and E. Rabinovici, Found. Phys. **33**, 145 (2003) [arXiv:hep-th/0211212].
- [8] G. T. Horowitz and E. Silverstein, arXiv:hep-th/0601032.
- [9] J. L. F. Barbon and E. Rabinovici, JHEP **0203**, 057 (2002) [arXiv:hep-th/0112173].
- [10] J. L. F. Barbon and E. Rabinovici, arXiv:hep-th/0407236.
- [11] A. Adams, X. Liu, J. McGreevy, A. Saltman and E. Silverstein, JHEP **0510**, 033 (2005) [arXiv:hep-th/0502021].
- [12] J. McGreevy and E. Silverstein, JHEP **0508**, 090 (2005) [arXiv:hep-th/0506130].
- [13] E. Silverstein, arXiv:hep-th/0602230.

- [14] D. J. Gross, M. J. Perry and L. G. Yaffe, Phys. Rev. D **25**, 330 (1982).
- [15] S. W. Hawking and D. N. Page, Commun. Math. Phys. **87**, 577 (1983).
- [16] J. W. York, Phys. Rev. D **33**, 2092 (1986).
- [17] J. Maldacena, Adv. Theor. Math. Phys. **2**, 231 (1998) [Int. J. Theor. Phys. **38**, 1113 (1999)] [arXiv:hep-th/9711200].
- [18] S. S. Gubser, I. R. Kelebanov and A. M. Polyakov, Phys. Lett. **B428**, 105 (1998)[arXiv:hep-th/9802109].
- [19] E. Witten, Adv. Theor. Math. Phys. **2**, 253 (1998) [arXiv:hep-th/9802150].
- [20] E. Witten, Adv. Theor. Math. Phys. **2**, 505 (1998) [arXiv:hep-th/9803131].
- [21] D. J. Gross and E. Witten, Phys. Rev. D **21**, 446 (1980).
- [22] G. T. Horowitz and J. Polchinski, Phys. Rev. D **55**, 6189 (1997) [arXiv:hep-th/9612146].
- [23] L. Alvarez-Gaume, C. Gomez, H. Liu and S. Wadia, Phys. Rev. D **71**, 124023 (2005) [arXiv:hep-th/0502227].
- [24] O. Aharony, J. Marsano, S. Minwalla, K. Papadodimas and M. Van Raamsdonk, Adv. Theor. Math. Phys. **8**, 603 (2004) [arXiv:hep-th/0310285].
- [25] T. Banks, M. R. Douglas, G. T. Horowitz and E. J. Martinec, arXiv:hep-th/9808016.
- [26] J. Crisostomo, R. Troncoso, and J. Zanelli, Phys. Rev. D **62**, 084013 (2000) [arXiv:hep-th/0003271].
- [27] R. G. Cai and K. S. Soh, Phys. Rev. D **59**, 044013 (1999) [arXiv:gr-qc/9808067].
- [28] Y. S. Myung, Phys. Lett. B **574**, 289 (2003) [arXiv:hep-th/0308191].
- [29] Y. S. Myung, Phys. Lett. B **624**, 297 (2005) [arXiv:hep-th/0506096].
- [30] Y. S. Myung, arXiv:hep-th/0603200.
- [31] D. Klemm, A. C. Petkou, G. Siopsis and D. Zanon, Nucl. Phys. B **620**, 519 (2002) [arXiv:hep-th/0104141].
- [32] E. P. Verlinde, arXiv:hep-th/0008140.

- [33] S. S. Gubser, Phys. Rev. D **63**, 084017 (2001) [arXiv:hep-th/9912001].
- [34] M. J. Duff and J. T. Liu, Phys. Rev. Lett. **85**, 2052 (2000) [Class. Quant. Grav. **18**, 3207 (2001)] [arXiv:hep-th/0003237].
- [35] V. P. Frolov, D. V. Fursaev and A. I. Zelnikov, Phys. Rev. D **54**, 2711 (1996) [arXiv:hep-th/9512184].
- [36] J. J. Atick and E. Witten, Nucl. Phys. B **310**, 291 (1988).
- [37] M. Kleban, M. Porrati and R. Rabadan, JHEP **0410**, 030(2004)[hep-th/0407192].
- [38] Y. S. Myung, Phys. Lett. B **638**, 515 (2006) [arXiv:gr-qc/0603051].
- [39] R. G. Cai, Y. S. Myung and N. Ohta, Class. Quant. Grav. **18**, 5429 (2001) [arXiv:hep-th/0105070].
- [40] G. W. Gibbons, M. J. Perry and C. N. Pope, Phys. Rev. D **72**, 084028 (2005) [arXiv:hep-th/0506233].
- [41] D. Klemm, A. C. Petkou and G. Siopsis, Nucl. Phys. B **601**, 380 (2001) [arXiv:hep-th/0101076].
- [42] L. Cappiello and W. Muck, Phys. Lett. B **522**, 139 (2001) [arXiv:hep-th/0107238].
- [43] G. J. Stephens and B. L. Hu, Int. J. Theor. Phys. **40**, 2183 (2001) [arXiv:gr-qc/0102052].
- [44] M. Berkooz, B. Pioline and M. Rozali, JCAP **0408**, 004 (2004) [arXiv:hep-th/0405126].
- [45] J. H. She, arXiv:hep-th/0512299.